

# SCIENTIFIC REPORTS



OPEN

## Electrical and mechanical switching of ferroelectric polarization in the 70 nm BiFeO<sub>3</sub> film

Liufang Chen<sup>1</sup>, Zhihao Cheng<sup>1</sup>, Wenting Xu<sup>1</sup>, Xiangjian Meng<sup>3</sup>, Guoliang Yuan<sup>1</sup>, Junming Liu<sup>2</sup> & Zhiguo Liu<sup>2</sup>

Received: 02 July 2015  
Accepted: 28 September 2015  
Published: 11 January 2016

Ferroelectric polarization switching and its domain evolution play a key role on the macroscopic electric properties of ferroelectric or piezoelectric devices. Mechanical switching has been reported recently in ~5 nm BaTiO<sub>3</sub> and PbZr<sub>0.2</sub>Ti<sub>0.8</sub>O<sub>3</sub> epitaxial films; however it is still a challenge for a mechanical force to switch polarization of a slightly thicker film in the same way as an electric field. Here, we report that the polarization of a 70 nm BiFeO<sub>3</sub> epitaxial film can be completely switched by a mechanical force, and its domain evolution is similar to that observed with electrical switching. With the gradual increase of the field/force, new domains nucleate preferentially at domain boundaries, the μm-size domains commonly decompose to a mass of nm-size domains, and finally they may reorganize to μm-size domains which undergo 180° polarization switching through multi steps. Importantly, the complete mechanical switching of polarization was also established in the (0 0 1) film with a smooth surface. Furthermore, either upward or downward polarization can be read out nondestructively by a constant current. Our study sheds light on prospective applications of ferroelectrics in the absence of an electric field, such as memory devices and other micro-electromechanical systems.

Ferroelectrics are widely used in electronic, sensing and machinery products, including energy harvesting devices<sup>1</sup>, actuators<sup>2</sup>, tuneable microwave devices<sup>3</sup>, and non-volatile memories<sup>4</sup>. The polarization switching and the corresponding domain evolution are very important for optimizing the ferroelectric and piezoelectric properties of such devices. For example, storing a data bit means increasing the size of one polar region at the expense of another in the non-volatile ferroelectric memory, and thus the motion of domain walls is critical to the applications<sup>5</sup>.

BiFeO<sub>3</sub> exists in a ferroelectric phase below ~813 °C and a canted anti-ferromagnetic phase below ~370 °C. It is a simple rhombohedrally-distorted cubic perovskite with polarization parallel to one of the four pseudo-cubic body diagonals [1 1 1]<sup>6</sup>. It shows a large remnant polarization ( $P_r$ , ~100 μC/cm<sup>2</sup>) along the [1 1 1] polar direction. There are four different structural variants in BiFeO<sub>3</sub>, leading to eight possible polarization directions and three (180°, 109° and 71°) domain walls<sup>7–10</sup>. Polarization switching and the corresponding domain evolution of (0 0 1) BiFeO<sub>3</sub> epitaxial films are important for enhancing their multiferroic properties. Although there are lots of reports about the polarization switching of the BiFeO<sub>3</sub> film under an electric field, we are still not clear about the domain evolution during the polarization switching period, especially those under a mechanical force.

Strain engineering can modify the properties of thin films using the stress from the substrates or an outer mechanical force. Epitaxial strain is widely used to manipulate the crystal lattice and then to optimize the piezoelectric and multiferroic properties in BiFeO<sub>3</sub> films<sup>8–13</sup>. In previous studies, a single domain could be induced in the as-grown BiFeO<sub>3</sub> film by epitaxial strain from the vicinal SrTiO<sub>3</sub> substrates<sup>10</sup>. Strain may be relaxed through the thickness of a film, however, ferroelectric properties can also be modified thanks to the coupling between strain gradient and polarization known as flexoelectricity. The mechanical switching of ferroelectric polarization has been reported in the 4.8 nm BaTiO<sub>3</sub> epitaxial film and the 5 nm PbZr<sub>0.2</sub>Ti<sub>0.8</sub>O<sub>3</sub> film<sup>14–16</sup>. However, it is still a challenge to switch the polarization of the slightly thicker ferroelectric film, especially the BiFeO<sub>3</sub> film with much larger coercive field than others.

<sup>1</sup>School of Materials Science and Engineering, Nanjing University of Science and Technology, Nanjing 210094, P. R. China. <sup>2</sup>National Laboratory of Solid State Microstructures, Nanjing University, Nanjing 210093, P. R. China. <sup>3</sup>National Laboratory for Infrared Physics, Shanghai Institute of Technical Physics, Chinese Academy of Sciences, Yu Tian Road 500, Shanghai 200083, P. R. China. Correspondence and requests for materials should be addressed to G.Y. (email: yuangoliang@njust.edu.cn)

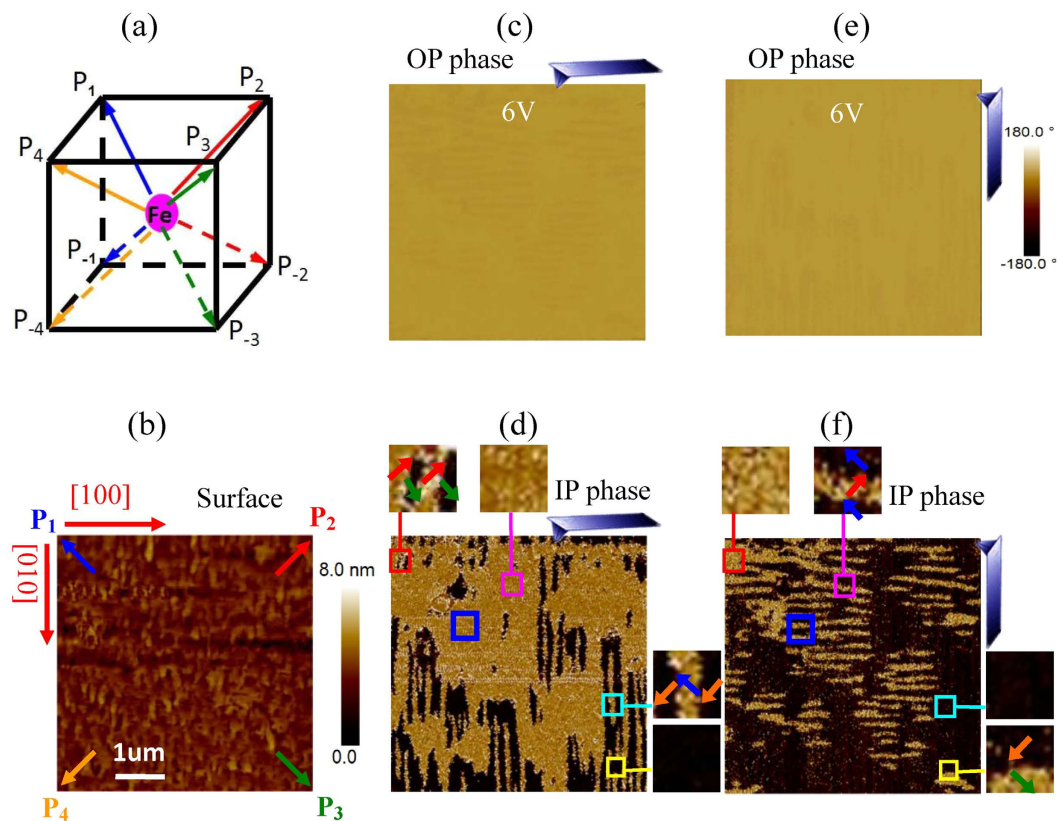


**Figure 1. The domain structure of BiFeO<sub>3</sub> film.** (a) The sketch of eight possible polarization orientations in a BiFeO<sub>3</sub> crystal cell; (b) the surface morphology, (c) out-of-plane (OP) and (d) in-plane (IP) phase images of the 6 V polarized regions; (e) the OP and (f) IP phase images of the same region observed with a 90°-rotated tip, where the [1 0 0] and [0 1 0] are crystal orientations, some domains with P<sub>1</sub>, P<sub>2</sub>, P<sub>3</sub> and P<sub>4</sub> are marked in (d) and (f), respectively.

Here the electrical and mechanical switching of ferroelectric polarization are achieved and the corresponding domain evolution is studied in the 70 nm (0 0 1) BiFeO<sub>3</sub> film with a smooth surface.

## Results

**Polarization orientations and domain structures.** The  $\mu\text{m}$ -size striped domains with 71° boundaries are introduced in the fully polarized 70 nm BiFeO<sub>3</sub> film on the (0 0 1) SrTiO<sub>3</sub> single-crystal substrate with La<sub>0.67</sub>Sr<sub>0.33</sub>MnO<sub>3</sub> buffer layer. There are eight different polarization orientations along the four diagonal lines of a BiFeO<sub>3</sub> crystal cell in Fig. 1a<sup>8,9</sup>. In the (0 0 1) BiFeO<sub>3</sub> film, the four upward polarizations (P<sub>1</sub>, P<sub>2</sub>, P<sub>3</sub> and P<sub>4</sub>) are toward the surface and the four downward polarizations (P<sub>-1</sub>, P<sub>-2</sub>, P<sub>-3</sub> and P<sub>-4</sub>) are toward the La<sub>0.67</sub>Sr<sub>0.33</sub>MnO<sub>3</sub> buffered layer. There is a nano-scale smooth surface in the  $5 \times 5 \mu\text{m}^2$  region of the as-grown BiFeO<sub>3</sub> film (Fig. 1b). After the as-grown film was polarized by 6 V from the La<sub>0.67</sub>Sr<sub>0.33</sub>MnO<sub>3</sub> layer (Fig. 1c,e), P<sub>1</sub>, P<sub>2</sub>, P<sub>3</sub> or P<sub>4</sub> were introduced (Fig. 1d,f). The tip can probe the polarization to be perpendicular to its cantilever in our system. P<sub>1</sub> and P<sub>2</sub> are yellow and P<sub>3</sub> and P<sub>4</sub> are black when the cantilever is along [1 0 0] in Fig. 1d, and P<sub>2</sub> and P<sub>3</sub> are yellow and P<sub>1</sub> and P<sub>4</sub> are black when the cantilever is along [0 1 0] in Fig. 1f<sup>13</sup>. It is found that striped domains with P<sub>2</sub>-P<sub>3</sub>, P<sub>3</sub>-P<sub>4</sub> or P<sub>4</sub>-P<sub>1</sub> periodic structure predominate. In previous studies, the polarization orientations and the domain sizes of BiFeO<sub>3</sub> film were successfully tailored by the static epitaxial strain from the film substrate<sup>8-13</sup>. Although thermal or epitaxial strain did not introduce striped domains in our as-grown film, it stabilized the periodic domain structure after the film was fully polarized.

**Electrical switching of ferroelectric polarization.** New domains nucleate preferentially at the previous domain boundaries under a negative bias. The P<sub>1</sub>-P<sub>2</sub> striped domains in the blue square of Fig. 1d-f are amplified and shown in Fig. 2a-d, where the inset is the corresponding surface morphology. There is a single domain in A, B, C, D, E and F regions, respectively. After the surface was scanned by a tip with -1.8 V bias, some new domains (e.g. B<sub>2</sub>, C<sub>2</sub>, D<sub>2</sub>, E<sub>2</sub> and F<sub>2</sub>) appeared at the previous P<sub>1</sub>-P<sub>2</sub> domain boundaries in Fig. 2e-h<sup>5</sup>. To our surprise, P<sub>1</sub>-P<sub>2</sub> boundaries were blurry, because the polarization was not unique at domain boundaries within the resolution of PFM. For the -2 V polarized region, the upward polarization becomes downward in over 94% regions (Fig. 2i-l). Many  $\mu\text{m}$ -size yellow and black domains do not have clear color contrast with each other, because they decompose to small or even nano-size domains due to various polarization switching routes in neighboring regions (e.g. A<sub>3</sub>)<sup>7</sup>. Nanodomains are beyond the resolution of PFM and thus they show a brown color

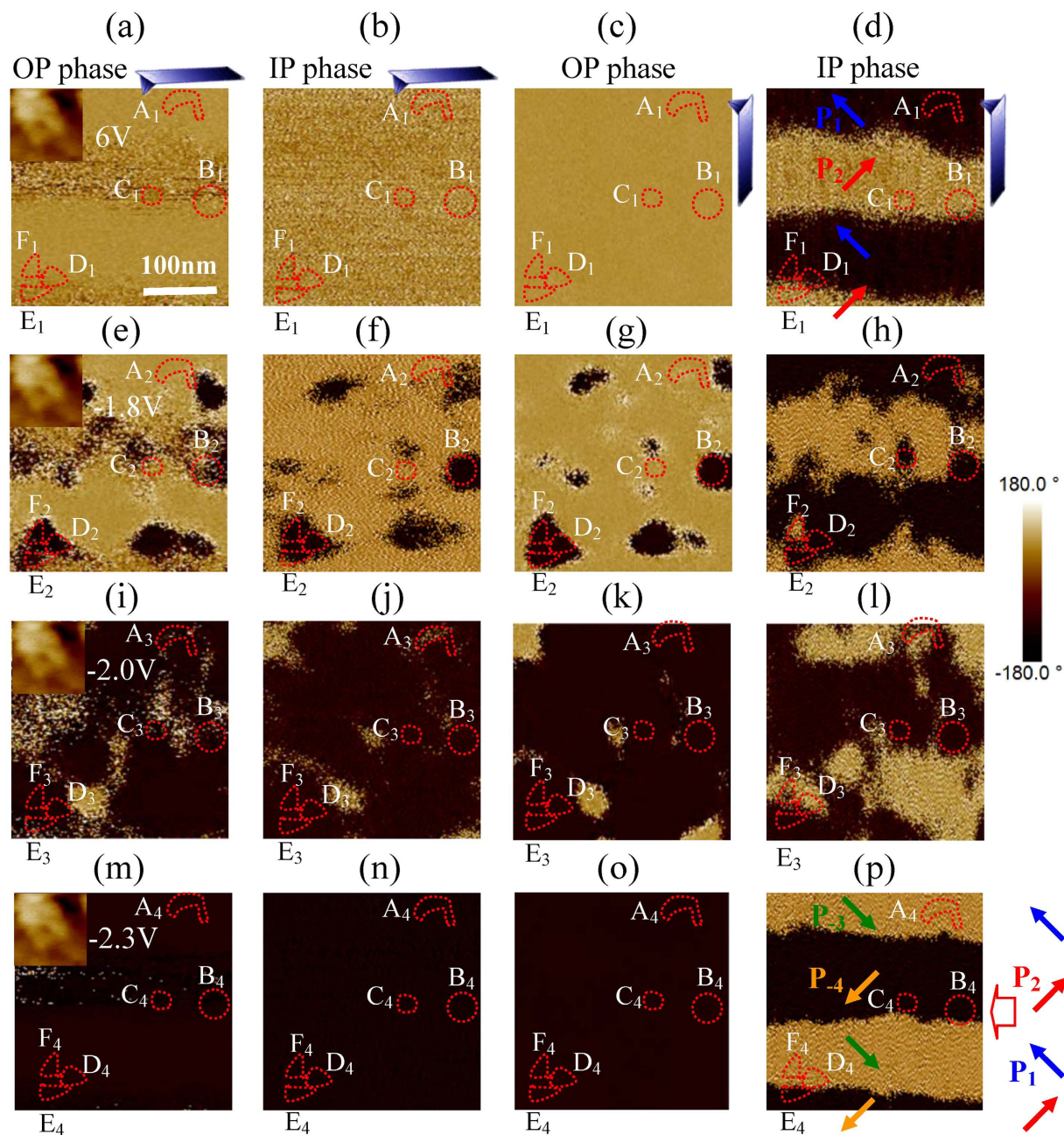


**Figure 2. The electrical switching of ferroelectric polarization.** The OP and IP phase images of the 6 V polarized area observed by a PFM tip with (a,b) 0° and (c,d) 90° rotations, and these phase images of the same area after it was polarized by (e–h) –1.8 V, (i–l) –2 V and (m–p) –2.3 V, where the inset is surface morphology and six independent regions are marked with A,B,C,D,E and F.

instead of the yellow or black seen in horizontal PFM images. The brown color did not come from the instrumental phase offset since the  $\mu\text{m}$ -size domains outside the –2 V polarized region still show yellow or black colors.

The nano-size domains assembled to  $\mu\text{m}$ -size  $P_{-3}/P_{-4}$  domains in the region of most previous striped domains when the poling field is larger than the coercive field ( $E_C$ ). After the film was polarized by –2.3 V again,  $P_{-3}$  and  $P_{-4}$  domains commonly exist in the regions of previous  $P_1$  and  $P_2$  domains (Fig. 2m–p), partially because the strain of  $P_1$ – $P_2$  striped domains is the same as that of the  $P_{-3}$ – $P_{-4}$  striped domains. That is to say, the  $P_1 \rightarrow P_{-3}$  or  $P_2 \rightarrow P_{-4}$  180° switching was realized through two steps (e.g.  $A_2(P_1) \rightarrow A_3(P_{-1}) \rightarrow A_4(P_{-3})$ ) here.

**Mechanical switching of ferroelectric polarization.** A mechanical force applied by the PFM tip can switch ferroelectric polarization through the flexoelectric effect<sup>14–17</sup>. The surface morphology of our  $\text{BiFeO}_3$  film is nm-scale smooth, as shown in Fig. 3a, which is important for the PFM tip to generate a large stress on the  $\text{BiFeO}_3$  film without inducing irreversible plastic damage. The mechanical switching has been investigated by scanning the  $1 \times 1 \mu\text{m}^2$  area of the upward polarized domain with the 30-nm-diameter tip under an incremental

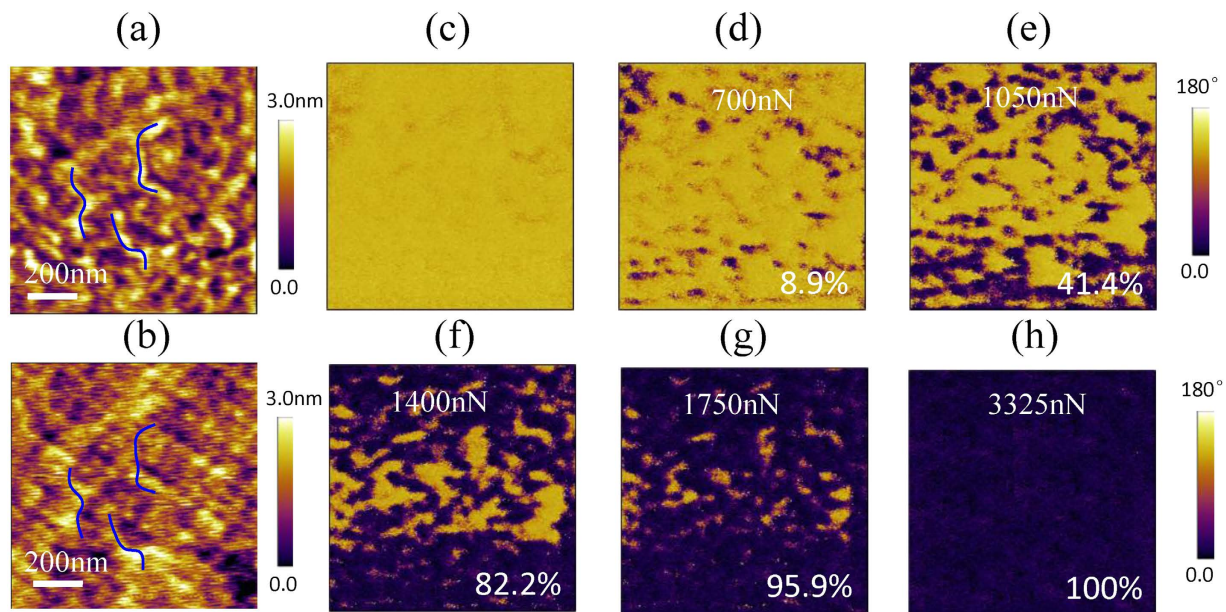


**Figure 3. The mechanical switching of ferroelectric polarization.** The surface morphology (a) before and (b) after it was scanned by the PFM tip with 3325 nN mechanical force. The OP phases image of the same region after it was scanned by the PFM tip with a force of (c) 140 nN, (d) 700 nN, (e) 1050 nN, (f) 1400 nN, (g) 1750 nN and (h) 3325 nN, where the percent is the ratio of area with downward polarization.

Electrical switching of polarization						
$A_1(P_1)$ (6V)	=	$A_2(P_1)$	$71^\circ$	$A_3(P_{-1})$	$109^\circ$	$A_4(P_{-3})$ (-2.3 V)
$B_1(P_2)$ (6V)	$180^\circ$	$B_2(P_{-4})$	$\approx$	$B_3(P_{-4})$	=	$B_4(P_{-4})$ (-2.3 V)
$C_1(P_2)$ (6V)	$71^\circ$	$C_2(P_1)$	$109^\circ$	$C_3(P_{-4})$	=	$C_4(P_{-4})$ (-2.3 V)
$D_1(P_1)$ (6V)	$109^\circ$	$D_2(P_{-4})$	$71^\circ$	$D_3(P_{-3})$	$\approx$	$D_4(P_{-3})$ (-2.3 V)
$E_1(P_2)$ (6V)	$180^\circ$	$E_2(P_{-4})$	=	$E_3(P_{-4})$	=	$E_4(P_{-4})$ (-2.3 V)
$F_1(P_1)$ (6V)	$180^\circ$	$F_2(P_{-3})$	$\approx$	$F_3(P_{-3})$	$\approx$	$F_4(P_{-3})$ (-2.3 V)
Mechanical switching of polarization						
$G_1(P_1)$ (6V)	$109^\circ$	$G_2(P_{-2})$	$\approx$	$G_3(P_{-2})$	$71^\circ$	$G_4(P_{-3})$ (1330 nN)
$H_1(P_1)$ (6V)	$109^\circ$	$H_2(P_{-2})$	$\approx$	$H_3(P_{-2})$	$71^\circ$	$H_4(P_{-3})$ (1330 nN)
$I_1(P_1)$ (6V)	=	$I_2(P_1)$	$\approx$	$I_3(P_1)$	$180^\circ$	$I_4(P_{-3})$ (1330 nN)
$J_1(P_4)$ (6V)	$109^\circ$	$J_2(P_{-3})$	$71^\circ$	$J_3(P_{-2})$	=	$J_4(P_{-2})$ (1330 nN)
$K_1(P_1)$ (6V)	$109^\circ$	$K_2(P_{-2})$	$\approx$	$K_3(P_{-2})$	$71^\circ$	$K_4(P_{-3})$ (1330 nN)

**Table 1. Different polarization switching routes of BiFeO<sub>3</sub> film under an electric field or a mechanical force.**

mechanical force from 700 to 3325 nN, with a corresponding change in the applied stress from 0.25 to 1.18 GPa. Note that, although the maximum local stress is very large, it is still well below the threshold for irreversible plastic damage of the BiFeO<sub>3</sub> surface (Fig. 3b). In the tip-stressed BiFeO<sub>3</sub> film, a strain gradient develops mainly along the film's normal, which introduces an asymmetric distribution of lattice deformation underneath the tip. This gives rise to a local electric field, i.e., the flexoelectric field, pointing to the substrate due to the flexoelectric effect<sup>18–20</sup>. The flexoelectric field is given by  $E_f = (f/\epsilon) \cdot (\partial e/\partial z)$ , where  $f$  is the flexoelectric tensor,  $\epsilon$  is the dielectric constant of the BiFeO<sub>3</sub> thin film,  $e$  is the strain due to the mechanical force of PFM tip, and  $z$  is the spatial coordinate along the film's normal<sup>14–17</sup>. The  $E_f$  increases with the increase of mechanical force, which breaks the symmetry in the ferroelectric potential of BiFeO<sub>3</sub> and makes the upward polarizations energetically unfavorable<sup>18–20</sup>.

The mechanical switching of polarization and its domain evolution are similar to those of the electrical switching. There is just upward polarization in the original image (Fig. 3c). When the mechanical force is 700 nN, the downward polarized domain starts to nucleate and then propagates. After the force of 700 nN, 1050 nN, 1400 nN, 1750 nN and 3325 nN had been applied by the PFM tip, the downward polarized domains were induced in the 8.9% (Fig. 3d), 41.4% (Fig. 3e), 82.2% (Fig. 3f), 95.9% (Fig. 3g) and 100% (Fig. 3h) region of total area, respectively. The downward polarized domains were stable after the sample had been kept for two days in air, which suggests the complete switching of polarization in 70 nm film.

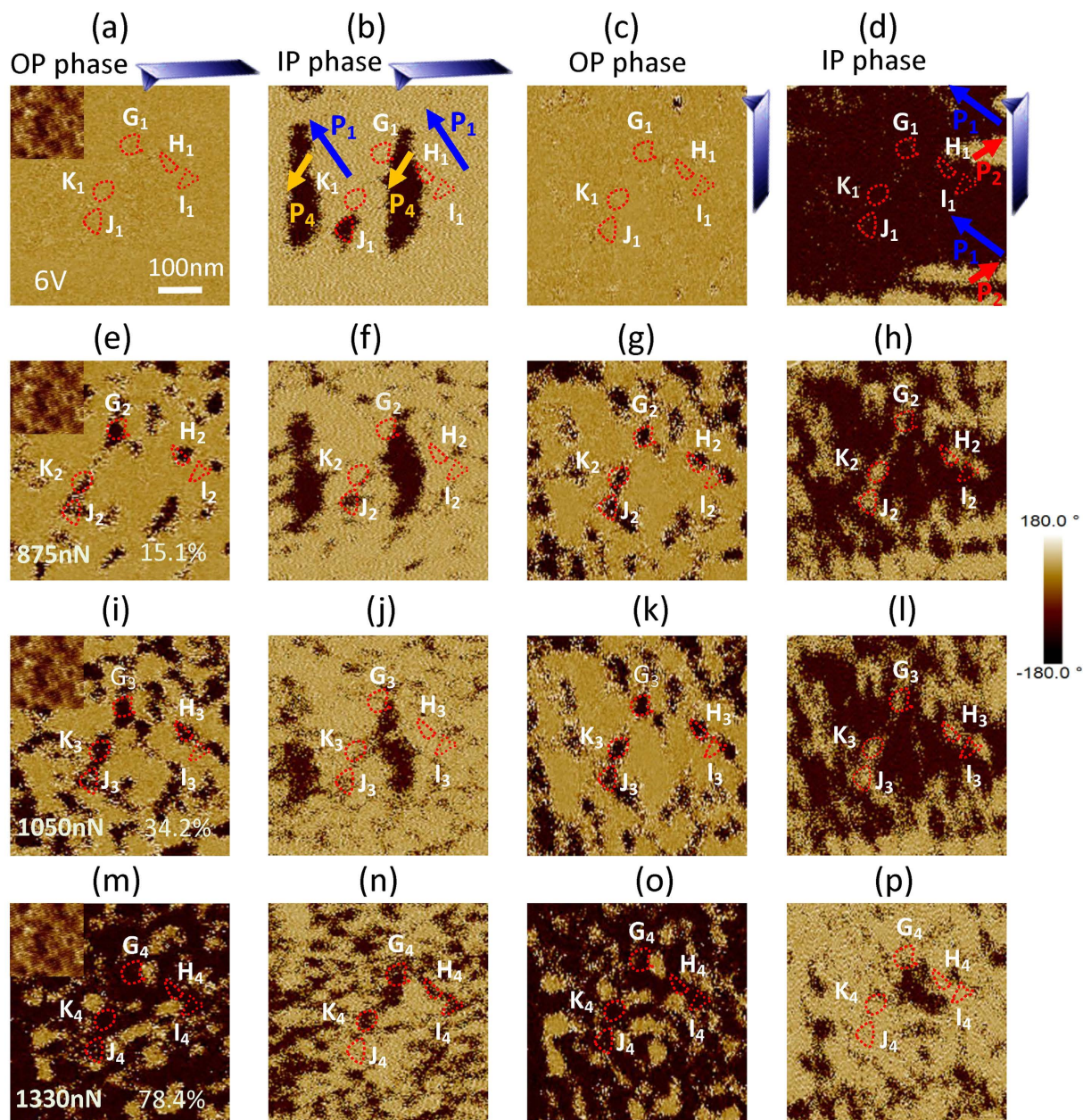


**Figure 4. The mechanical switching of ferroelectric polarization.** The OP and IP phase images of the 6 V polarized area observed by a PFM tip with (a,b)  $0^\circ$  and (c,d)  $90^\circ$  rotations, and the images of the same area after it was polarized by a mechanical force of (e–h) 875 nN, (i–l) 1050 nN, (m–p) 1330 nN, where the inset is the surface morphology, the five independent regions are marked with G,H,I,J and K, and the percent is the ratio of area with downward polarization.

## Discussion

Table 1 summarizes the possible routes of polarization switching triggered by an electric field (Fig. 2) or a mechanical force (Fig. 4). According to previous phase-field calculation, direct  $180^\circ$  polarization switching is not kinetically favorable because of the high activation barrier. Instead, the ferroelastic relaxation-mediated  $180^\circ$  switching path through  $71^\circ$  switching is expected<sup>21</sup>. Not only the polarization direction but also the direction of lattice distortion changes at  $109^\circ$  and  $71^\circ$  ferroelastic domain walls<sup>7–10</sup>. There is an easy magnetization plane for the orientation of the magnetic moments, which is always perpendicular to the ferroelectric polarization orientation. Either  $109^\circ$  or  $71^\circ$  polarization switching changes the orientation of the easy magnetization plane<sup>8–10</sup>. The realization of permanent magnetoelectric coupling in the single-phase BiFeO<sub>3</sub> requires ferroelastic ( $71^\circ$ ,  $109^\circ$ ) rather than ferroelectric ( $180^\circ$ ) domain switching<sup>21–23</sup>. That is to say, there may exist transient magnetoelectric coupling during the  $180^\circ$  polarization switching which is commonly composed of a  $71^\circ$  and a  $109^\circ$  polarization switching. In the intermediate stage of the  $180^\circ$  switching, there are several possible polarization orientations, and thus tiny domains are the most popular.

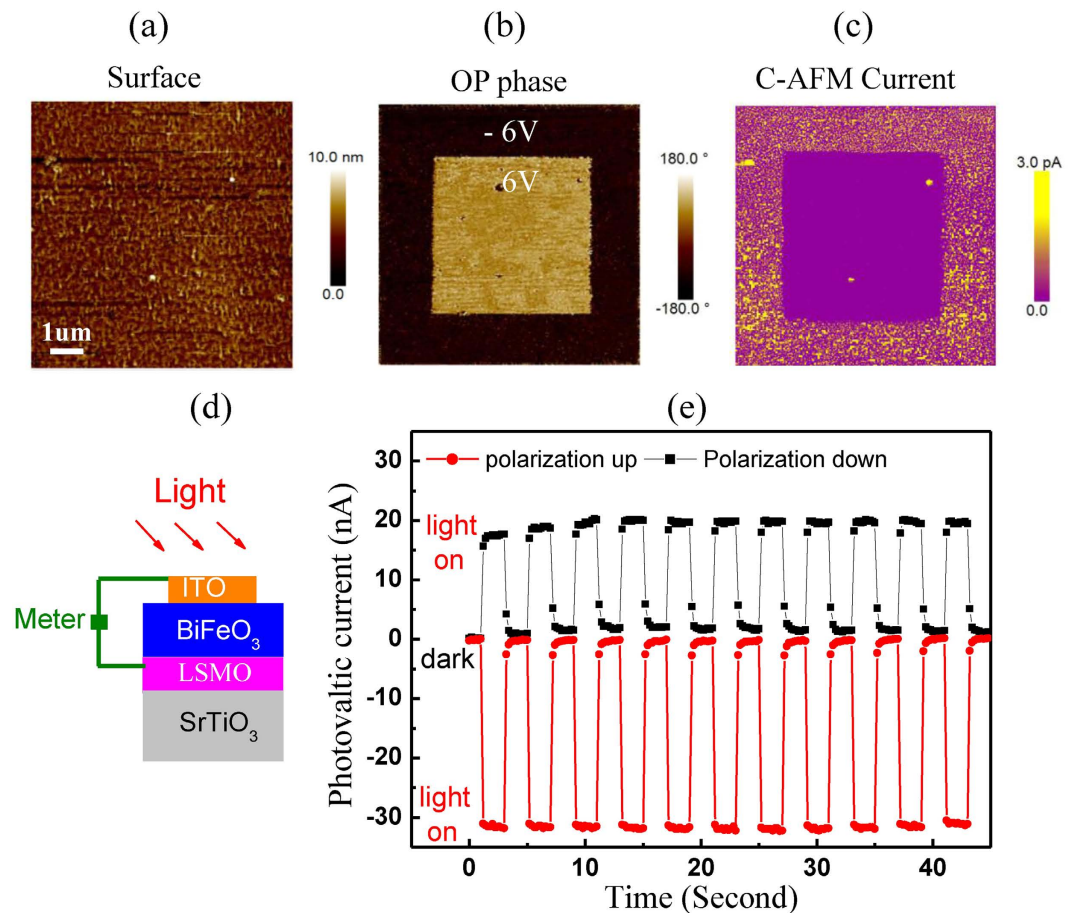


**Figure 5. The ferroelectric polarization is nondestructively read out.** (a) The surface morphology, (b) the OP phase image and (c) the conductive image with 1 V bias after the film were polarized by 6 V and  $-6$  V bias, respectively. (d) The sketch of photovoltaic measurement. (e) The photovoltaic current of BiFeO<sub>3</sub> with upward or downward polarization when light illuminates the BiFeO<sub>3</sub> surface or not.

Although the  $\sim 70$  nm BiFeO<sub>3</sub> film shows a much higher coercive field than that of the BaTiO<sub>3</sub> film with similar thickness, its polarization was completely switched by a 3325 nN force. Recently, the epitaxial strain from substrate is widely used to tailor domain type or introduce self-polarization in BiFeO<sub>3</sub><sup>8–13</sup>. Besides, flexoelectricity also plays an important role in the self-polarized direction in BiFeO<sub>3</sub> film and ceramics<sup>24,25</sup>. Nowadays the inhomogeneous strain introduced by PFM tip can switch ferroelectric polarization of the 70 nm BiFeO<sub>3</sub> film and the mechanical switching of polarization is the same as the electrical switching. In addition to polarization switching, the tetragonal-rhombohedral phase transition can be introduced through an electric field or a mechanical force in a  $> 50$  nm BiFeO<sub>3</sub> film with morphotropic phase boundaries on LaAlO<sub>3</sub> substrate<sup>11,13,26,27</sup>. Although the mechanical force from AFM tip is large enough to trigger these polarization switching and phase transition indeed, other factors such as the epitaxial strain from substrate or the built-in electric field near the film interface may play an important role on these changes. This work is important for more applications since it is much easier to prepare and measure the  $\sim 70$  nm ferroelectric films than the  $\sim 5$  nm films<sup>14–17</sup>.

The domain evolution due to the mechanical switching is similar to that of the electrical switching. The domain evolution under a mechanical force is clearly observed and its polarization switching routes are identified accordingly. The  $\mu\text{m}$ -size  $P_1$ – $P_4$  and  $P_1$ – $P_2$  striped domains were formed in Fig. 4a–d. There is a single domain in  $G(P_1)$ ,  $H(P_1)$ ,  $I(P_1)$ ,  $J(P_4)$  and  $K(P_1)$  regions, respectively. With the mechanical force increasing gradually from 875 to 1330 nN, new tiny domains nucleate at the boundaries of  $\mu\text{m}$ -size domains, and then more and more  $\mu\text{m}$ -size domains decompose to nm-size domains due to different polarization switching routes (Fig. 4e–p). Polarization of G, H, J and K first has  $71^\circ/109^\circ$  switching and then  $109^\circ/71^\circ$  switching<sup>21–23</sup>, e.g.  $G_1(P_1) \rightarrow G_2(P_{-2}) \rightarrow G_4(P_{-3})$  and  $J_1(P_4) \rightarrow J_2(P_{-3}) \rightarrow J_3(P_{-2})$ . As a result, the  $180^\circ$  polarization switching was achieved with two steps. The routes of these regions are shown in Table 1.

Ferroelectric polarization can be nondestructively read-out without another polarization switching in our BiFeO<sub>3</sub> film. The regions with upward and downward polarization were polarized by a  $\pm 6$  V tip bias (Fig. 5a–b), and these regions were characterized by a conductive AFM tip with 1 V bias. It is noted that 1 V is much lower than the coercive voltage ( $V_C$ ) of  $\pm 2.3$  V which corresponds to the  $E_C$  of 38 kV/mm. The region with downward polarization shows much higher current than the region with upward polarization (Fig. 5c). Therefore the leakage current under a  $< V_C$  voltage can read out information in a nondestructive way<sup>28–29</sup>. Oxygen vacancies are typical

n-type dopant in BiFeO<sub>3</sub> film. There is a depletion layer at the interface between the p-type La<sub>0.67</sub>Sr<sub>0.33</sub>MnO<sub>3</sub> interlayer and the n-type BiFeO<sub>3</sub> film. The downward polarization increases the leakage current through narrowing the depletion layer at the La<sub>0.67</sub>Sr<sub>0.33</sub>MnO<sub>3</sub>/BiFeO<sub>3</sub> interface while the upward polarization decreases the leakage current through widening the depletion layer<sup>28–31</sup>. Furthermore, we measured the intrinsic photovoltaic effect of the BiFeO<sub>3</sub> films with 300- $\mu$ m-diameter transparent ITO electrodes which was illuminated by a visible light ( $\sim 100$  mW/cm<sup>2</sup>) (Fig. 5d). The short-circuit current ( $I_{sc}$ ) direction is always opposite to the polarization direction in Fig. 5e. The  $I_{sc}$  after downward poling was 20 nA, whereas the  $I_{sc}$  after upward poling was about  $-30$  nA<sup>31</sup>. The  $I_{sc}$  can be switched by polarization flipping. In addition, there is no obvious photocurrent degradation when the  $I_{sc}$  was measured during eleven on-and-off cycles of the illumination light. Such good retention and high stability over multiple cycles suggest that the polarization status can be nondestructively read out through the analysis of  $I_{sc}$ .

In summary, the electrical switching of polarization in the  $\sim 70$  nm epitaxial BiFeO<sub>3</sub> film is similar to that of mechanical switching. The 180° polarization switching is commonly completed with two steps. At first, a  $\mu$ m-size domain decomposes to nano-size domains due to the 71°/109°/180° polarization switching, and then they merge to a  $\mu$ m-size domain due to the other 109°/71°/0° switching. Most importantly, the upward polarization can be switched downward with a mechanical force even in the  $\sim 70$  nm BiFeO<sub>3</sub> film, and then the polarization status can be nondestructively read out through the analysis of constant current.

## Methods

**Thin film fabrication.** BiFeO<sub>3</sub> ( $\sim 70$  nm) epitaxial films and La<sub>0.67</sub>Sr<sub>0.33</sub>MnO<sub>3</sub> ( $\sim 70$  nm) buffer layers were grown on commercial (0 0 1) SrTiO<sub>3</sub> substrates using pulsed laser deposition (PLD) at 630 °C and 16 Pa oxygen pressure inside the chamber. The wavelength, frequency and energy per pulse of KrF excimer laser were 248 nm, 1 Hz and 60 mJ. After that, the as-grown samples were kept at 630 °C and 1000 Pa oxygen pressure for 30 minutes in order to reduce oxygen vacancies, and then they were cooled down at 5 °C per minute to 300 °C. For photovoltaic measurement, indium tin oxide (ITO, In<sub>2</sub>O<sub>3</sub>:SnO<sub>2</sub>=9:1) top electrodes with 300  $\mu$ m diameter were grown on the BiFeO<sub>3</sub> film surface at room temperature using PLD.

**Electrical measurements.** The surface morphology, out-of-plane (OP) phase, in-plane (IP) phase and amplitude images were studied by using the commercial atomic force microscope (AFM, Bruker multimode 8 or Asylum Research Cypher) with a piezoelectric force microscopy (PFM) mode. The conductive AFM tip is either Bruker MESP-RC with 35 nm tip radius or Nanoworld EFM with 30 nm tip radius. The spatially resolved conductance image was measured with the conductive AFM at 1 V sample bias (Bruker multimode 8). The photovoltaic current is measured with a Keithley 2635 multimeter when the film surface was illuminated by the light of a xenon lamp at 100 mW/cm<sup>2</sup>.

## References

- Jung, J. H. *et al.* Lead-free NaNbO<sub>3</sub> nanowires for a high output piezoelectric nanogenerator. *ACS Nano* **5**, 10041–10046 (2011).
- Chang, C., Tran, V. H., Wang, J., Fuh, Y.-K. & Lin, L. Direct-write piezoelectric polymeric nanogenerator with high energy conversion efficiency. *Nano Lett.* **10**, 726–731 (2010).
- Lee, C.-H. *et al.* Exploiting dimensionality and defect mitigation to create tunable microwave dielectrics. *Nature* **502**, 532–536 (2013).
- Scott, J. F. & Paz de Araujo, C. A. Ferroelectric memories. *Science* **246**, 1400–1405 (1989).
- Shin, Y. H., Grinberg, I., Chen, I. W. & Rappe, A. M. Nucleation and growth mechanism of ferroelectric domain-wall motion. *Nature* **449**, 881–884 (2007).
- Wang, J. *et al.* Epitaxial BiFeO<sub>3</sub> Multiferroic Thin Film Heterostructures. *Science* **299**, 1719–1722 (2003).
- Shafer, P. *et al.* Planar electrode piezoelectric force microscopy to study electric polarization switching in BiFeO<sub>3</sub>. *Appl. Phys. Lett.* **90**, 202909 (2007).
- Chu, Y.-H. *et al.* Electric-field control of local ferromagnetism using a magnetoelectric multiferroic. *Nat Mater* **7**, 478–482 (2008).
- Zhao, T. *et al.* Electrical control of antiferromagnetic domains in multiferroic BiFeO<sub>3</sub> films at room temperature. *Nat Mater* **5**, 823–829 (2006).
- Chu, Y.-H. *et al.* Domain Control in Multiferroic BiFeO<sub>3</sub> through Substrate Vicinality. *Adv. Mater.* **19**, 2662–2666 (2007).
- Zeches, R. J. *et al.* A Strain-Driven Morphotropic Phase Boundary in BiFeO<sub>3</sub>. *Science* **326**, 977–980 (2009).
- Cruz, M. P. *et al.* Strain Control of Domain-Wall Stability in Epitaxial BiFeO<sub>3</sub> (110) Films. *Phys. Rev. Lett.* **99**, 217601 (2007).
- You, L. *et al.* Characterization and Manipulation of Mixed Phase Nanodomains in Highly Strained BiFeO<sub>3</sub> Thin Films. *ACS Nano* **6**, 5388–5394 (2012).
- Lu, H. *et al.* Mechanical Writing of Ferroelectric Polarization. *Science* **336**, 59–61 (2012).
- Lu, H. *et al.* Mechanically-Induced Resistive Switching in Ferroelectric Tunnel Junctions. *Nano Lett.* **12**, 6289–6292 (2012).
- Guo, E. J., Roth, R., Das, S. & Dorr, K. Strain induced low mechanical switching force in ultrathin PbZr<sub>0.2</sub>Ti<sub>0.8</sub>O<sub>3</sub> films. *Appl. Phys. Lett.* **105**, 012903 (2014).
- Baek, S. H. *et al.* Ferroelastic switching for nanoscale non-volatile magnetoelectric devices. *Nat Mater* **9**, 309–314 (2010).
- Baek, S. H. *et al.* The Nature of Polarization Fatigue in BiFeO<sub>3</sub>. *Adv. Mater.* **23**, 1621–1625 (2011).
- Balke, N. *et al.* Deterministic control of ferroelastic switching in multiferroic materials. *Nature Nanotechnology* **4**, 868–875 (2009).
- Wen, Z. *et al.* Mechanical switching of ferroelectric polarization in ultrathin BaTiO<sub>3</sub> films: The effects of epitaxial strain. *Appl. Phys. Lett.* **104**, 042907 (2014).
- Zubko, P., Catalan, G., Buckley, A., Welche, P. R. L. & Scott, J. F. Strain-gradient-induced polarization in SrTiO<sub>3</sub> single crystals. *Phys. Rev. Lett.* **99**, 167601 (2007).
- Catalan, G., Noheda, B., McAneney, J., Sinnamon, L. J. & Gregg, J. M. Strain gradients in epitaxial ferroelectrics. *Phys. Rev. B* **72**, 020102 (2005).
- Catalan, G., Sinnamon, L. J. & Gregg, J. M. The effect of flexoelectricity on the dielectric properties of inhomogeneously strained ferroelectric thin films. *J. Phys. Conder. Matter.* **16**, 2253–2264 (2004).
- Chen, X. M. *et al.* Temperature Gradient Introduced Ferroelectric Self-Poling in BiFeO<sub>3</sub> Ceramics. *J. Amer. Ceram. Soc.* **96**, 3788–3792 (2013).
- Jeon, B. C. *et al.* Flexoelectric Effect in the Reversal of Self-Polarization and Associated Changes in the Electronic Functional Properties of BiFeO<sub>3</sub> Thin Films. *Adv. Mater.* **25**, 5643–5649 (2013).

26. Heo, Y., Jang, B. K., Kim, S. J. & Seidel, J. Nanoscale mechanical softening of morphotropic BiFeO<sub>3</sub>, *Adv. Mater.* **26**, 7568–7572 (2015).
27. Li, Y. J. *et al.* Mechanical switching of nanoscale multiferroic phase boundaries, *Adv. Funct. Mater.* **25**, 3405–3413 (2015).
28. Jiang, A. Q. *et al.* A Resistive Memory in Semiconducting BiFeO<sub>3</sub> Thin-Film Capacitors. *Adv. Mater.* **23**, 1277–1281 (2011).
29. Yuan, G. L. & Wang, J. L. Evidences for the depletion region induced by the polarization of ferroelectric semiconductors. *Appl. Phys. Lett.* **95**, 252904 (2009).
30. Choi, T., Lee, S., Choi, Y. J., Kiryukhin, V. & Cheong, S.-W. Switchable Ferroelectric Diode and Photovoltaic Effect in BiFeO<sub>3</sub>. *Science* **324**, 63–66 (2009).
31. Yi, H. T., Choi, T., Choi, S. G., Oh, Y. S. & Cheong, S.-W. Mechanism of the Switchable Photovoltaic Effect in Ferroelectric BiFeO<sub>3</sub>. *Adv. Mater.* **23**, 3403–3407 (2011).

### Acknowledgements

The work is supported by the National Natural Science Foundation of China (11134004, 11234005, 51472118 and 11374320).

### Author Contributions

G.L.Y conceived the experiments, L.F.C. and W. T. X. grew the films, L.F.C and Z.H.C. performed the conductive AFM and PFM measurements. G.L.Y., X.J.M., J.M.L. and Z.G.L. analyzed data and then co-wrote the manuscript.

### Additional Information

**Competing financial interests:** The authors declare no competing financial interests.

**How to cite this article:** Chen, L. *et al.* Electrical and mechanical switching of ferroelectric polarization in the 70 nm BiFeO<sub>3</sub> film. *Sci. Rep.* **6**, 19092; doi: 10.1038/srep19092 (2016).



This work is licensed under a Creative Commons Attribution 4.0 International License. The images or other third party material in this article are included in the article's Creative Commons license, unless indicated otherwise in the credit line; if the material is not included under the Creative Commons license, users will need to obtain permission from the license holder to reproduce the material. To view a copy of this license, visit <http://creativecommons.org/licenses/by/4.0/>